

Dependency of temperature on polarization in CH₄/N₂ dielectric barrier discharge plasma: A crude assumption

Abhijit Majumdar,^{1,a)} Basudev Ghosh,² and Rainer Hippler¹

¹*Institut of Physics, University of Greifswald, Felix Hausdorff Strasse 6, 17489 Greifswald, Germany*

²*Jadavpur University, Kolkata 700032, West Bengal, India*

(Received 2 August 2010; accepted 4 October 2010; published online 9 November 2010)

We have investigated the variations of polarization (P) and the temperature (ΔT) at the electrode surfaces during the deposition of C–N layer in CH₄/N₂ (1:2) dielectric barrier discharge plasma. The reactive deposition process influences the surface temperature, polarization, and the value of the *in situ* dielectric constant. We have developed a crude model that correlates the surface temperature and surface polarization with thin film properties. We assume that during the thin film deposition process, the atomic mean kinetic energy is equal to the electrostatic energy stored in the electrode surface area. Theoretically estimated temperature is found to agree well with the experimental results. However, the linear model thus developed cannot be used to explain the phenomena in the interfacial polarization stage that requires a nonlinear theory. © 2010 American Institute of Physics. [doi:10.1063/1.3505111]

I. INTRODUCTION

The plasma assisted thin film deposition is currently the most promising field of deposition techniques.^{1–11} It is an important and growing field in plasma technology. In order to improve the film depositions (i.e., deposition rate, film quality, and film uniformity), the numerical modeling of the plasma discharge can be of much use in achieving a better understanding of the various factors involved in the film deposition process. The properties of the deposited film are influenced by the plasma characteristics and the specific deposition conditions such as power, gas mixture and gas flow. Some models^{12–18} have been developed for lower moderate pressure systems and for thermal plasmas where the reaction mechanisms are governed by the neutral gas temperature. In plasma deposition, the growth of low-molecular-weight molecules (monomers) into high-molecular-weight molecules (polymers) occurs with the assistance of the plasma energy, which involves energetic electrons, ions, and radicals.¹⁹ Plasma polymerization is a thin film forming process, where thin films are directly deposited on surfaces of the substrate without any fabrication. In CH₄/N₂ or other hydrocarbons (i.e., C₂H₄/Ar/N₂, C₂H₆/Ar/N₂, etc.), the gas mixture plasma and the gas molecules gain energy from the plasma through inelastic collision and fragmented into energetic smaller molecules. The smaller molecules recombine to form a larger molecule and polymers are deposited at the surface of the substrates. The depositing polymers are constantly irradiated by the plasma until the polymerization process is completed. If the deposited polymers are subject to an interaction of the plasma the polymers may degrade to some extent. During the discharge the layer thickness increases and the layer properties such as dielectric constant, polariza-

tion of the surface, effective capacitance of the electrode surface, temperature, etc. change with time.

In our experiment, we have observed how the plasma polarization changes with time. It has also been observed that the dielectric properties of C–N layer taken out after the deposition process are different from that during the plasma deposition process. This is an effect introduced by the reactive nature of the plasma deposition process and the local dielectric relaxation of the deposited molecules. Both the temperature and polarization of the growing films are the results of plasma-surface interaction and are expected to be somehow interrelated. Thus it is important to know about the temperature profile of the electrodes surface area during the thin film deposition.

Due to the electric field in the system, the energy is mainly dissipated by inelastic collisions of electrons and electromagnetic interaction via excitation, dissociation, and ionization to the particles of the processed gas that is partly deposited at electrode surface. Some of the electrons in the plasma also transfer energy to the polymers through electrostatic interaction followed by ionization or excitation of the polymers. It leads to the formation of free radicals at surface of the polymers.

The strength and range of the electric force and the good conductivity of plasmas usually ensure that the densities of positive and negative charges in any sizeable region are equal (“quasineutrality”). The plasma that has a significant excess of charge density or is in the extreme case, composed of only a single species, is called non-neutral plasma. DBD plasma is known as non-neutral plasma but we assume that during the deposition process, the plasma attains an equilibrium condition. In such plasma, electric fields play a dominant role. In the DBD discharge that is apart from the applied electric field, there is a displacement current (between the electrodes) at every discharge cycle and that also enhances the charge accumulation on electrode surface area. In such circumstances, for simplicity, we assume that the mean ki-

^{a)} Author to whom correspondence should be addressed. Electronic mail: majumdar@physik.uni-greifswald.de. Tel. No.: +493834864784. FAX: +493834864701.

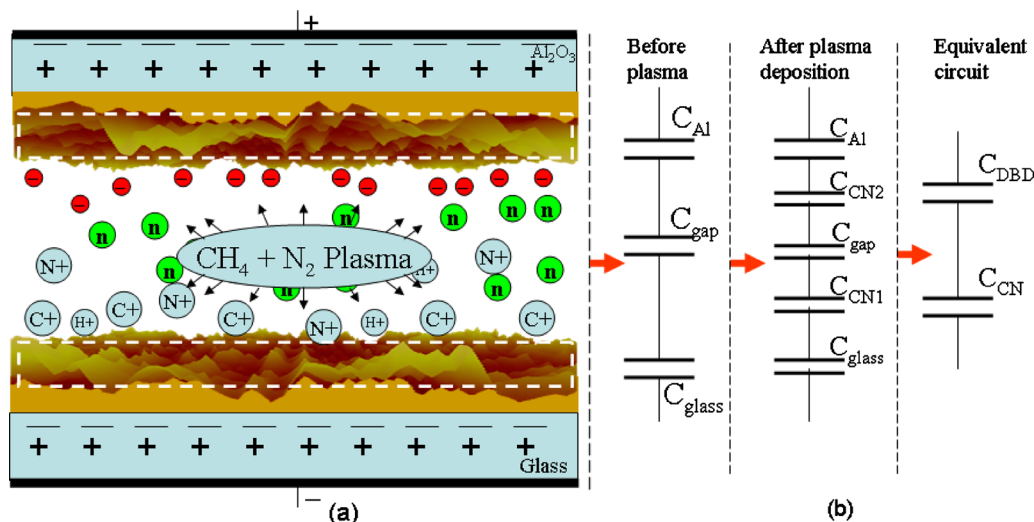


FIG. 1. (Color online) (a) Schematics of dielectric barrier discharge configuration. Upper electrode is connected to the high voltage connection and lower one is grounded (Ref. 5). (b) Equivalent circuit of the DBD system where it has been classified in three different sections: before plasma, after plasma deposition, and final equivalent circuit.

netic energy of the molecules during the discharge is roughly equal to the energy stored in the electrostatic field that is distributed over the surface of the barrier discharge electrodes. Actually, the mean kinetic energy of the molecules is certainly smaller than the field energy, since there exists still other energy dissipation channels. However the experimental results are found to fit well with the assumption.

So far, as we are aware of the literature, there is no concrete model or data for temperature/polarization measurement in atmospheric dielectric barrier discharge (DBD) plasma. This is the first time we attempt to correlate the polarization and temperature in reactive DBD plasma. As we are dealing with the near atmospheric pressure dielectric barrier discharge plasma, the number of collision is high and the mean free paths of the atoms and electrons (etc.) are very small. So, in such case, it is more realistic to consider the gas temperature rather than electron or ion temperature. Moreover, the gas temperature is governed by the mean kinetic energy of the atoms. So, to support our assumption, we did the corresponding experiments and interestingly the results fit well with our assumption. However still there is scope for further detailed study. Applying the assumption as stated above, we have investigated the variation of polarization (P) and the temperature (ΔT) at the electrode surfaces during the deposition of C–N layer in CH_4/N_2 (1:2) dielectric barrier discharge plasma. In this paper, it is shown that the change in temperature at the electrode surface depends on the value of polarization and the *in situ* dielectric constant of the deposited layer. Theoretically, the estimated temperature is also compared with the experimental results.

II. EXPERIMENTAL

Figure 1 shows the schematic view of our DBD system and its equivalent capacitance circuit configuration that is similar to that used in Ref. 20. It essentially consists of two electrodes (upper electrode- Al_2O_3 and lower electrode glass) placed inside a vacuum chamber. The gap between the elec-

trodes is 0.20 cm. The upper electrode is connected to a home-built high voltage power supply, while the lower electrode is grounded. The reaction chamber has to be evacuated by a membrane pump up to 1 mbar before any experiment. After filling up the chamber with the gas mixture up to 300–500 mbar as per requirement, it is isolated from the surroundings by using needle valve arrangement. A capillary tube with diameter 0.1 mm is connected between the mass spectrometer and the reaction chamber. A second turbomolecular pump (Balzers 071P) is used to create the pressure gradient in between chamber and the mass spectrometer. The water flow should be on during the discharge to cool down the mass spectrometer filament and the high voltage transformer coil and amplifier system. The grounding and earthing should be properly checked before discharge. Once the discharge is on the voltage can be vary from 4 to 15 kV (peak to peak) and the frequency can be vary from 2 to 7.5 kHz. The high voltage power supply has a signal generator delivering a sinusoidal output that is fed into an audio amplifier. The amplifier can be operated at power levels up to 500 W. A high voltage around 9.6 kV (peak to peak) and of frequency 5 kHz is applied between the electrodes. The electrical power under these conditions is in the range of 1–3 W.

To characterize the overall discharge behavior, an equivalent electric circuit conception can be used. As long as the gap voltage is smaller than the ignition voltage, there is no discharge activity and the device behaves like a series combination of three capacitors; the capacitance of upper electrode $C_{\text{Al}_2\text{O}_3}$, the gap capacitance C_{gap} , and the capacitance of lower electrode C_{glass} [compare Fig. 1(a)]. Then the total capacitance C_{DBD} is given by the expression

$$\frac{1}{C_{\text{DBD}}} = \frac{1}{C_{\text{Al}_2\text{O}_3}} + \frac{1}{C_{\text{gap}}} + \frac{1}{C_{\text{glass}}}. \quad (1)$$

After the breakdown discharge [Fig. 1(b)], CH_4/N_2 mixture breaks down and thin layer of CNx is deposited on the electrodes area. We refer the thin layers as CN1 and CN2 (even-

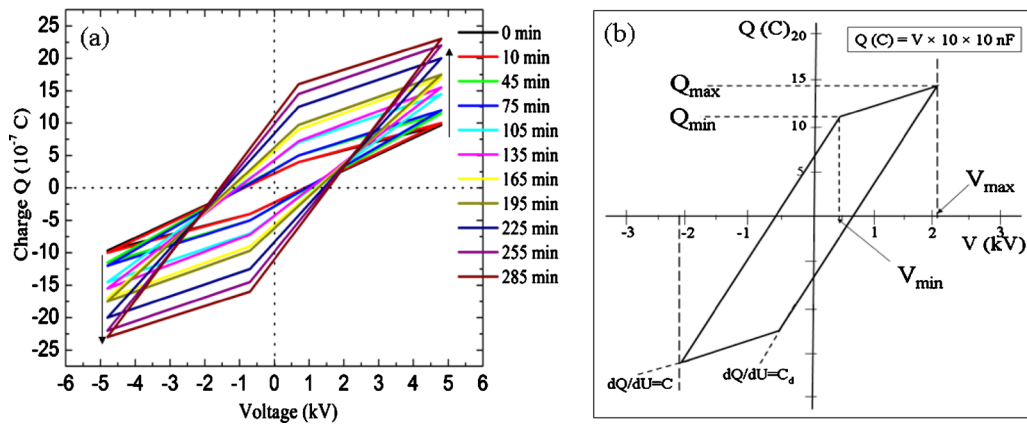


FIG. 2. (Color online) (a) Charge-voltage characteristic (Lissajous) curve of CH_4/N_2 (1:2) dielectric barrier discharge plasma for different plasma processing times. The area of the parallelogram is related to the electric power dissipated during the each cycle. (b) A typical Q-V (Lissajous) curve of hydrocarbon DBD plasma.

tually, the thickness of CN1 and CN2 is considered to be the same). These thin layers will also act as capacitor and now the whole DBD system behaves like a series combination of five capacitors. Thus,

$$\frac{1}{C_{\text{Equivalent}}} = \frac{1}{C_{\text{Al}_2\text{O}_3}} + \frac{1}{C_{\text{CN1}}} + \frac{1}{C_{\text{gap2}}} + \frac{1}{C_{\text{glass}}} + \frac{1}{C_{\text{CN2}}}. \quad (2)$$

The CN layer thickness is very small ($\sim 1 \mu\text{m}$) compared to the air gap1 (2 mm). So the air gap1 and gap2 can be considered as the same. So after CN film deposition, the equivalent capacitance of the DBD system can be expressed as follows:

$$\frac{1}{C_{\text{Equivalent}}} = \frac{1}{C_{\text{DBD}}} + \frac{1}{C_{\text{CN}}}. \quad (3)$$

The term C_{DBD} (capacitance of the DBD system, when there is no deposition) is constant since electrodes are unchanged and the electrodes gap is same as before (as the deposited thin layer is negligibly small compared to air gap). So, the change in equivalent capacitance will only depend on the capacitance of the deposited thin layer (i.e., C_{CN}).

Equations (1)–(3) help us to get an overview of the equivalent capacitor circuit of our DBD system. We have used the typical charge-voltage characteristic curve (Lissajous curve) to find out the net charge deposited for a given applied voltage during the plasma deposition. In Fig. 2(a), x- and y-axes represent the applied voltage (kilovolt) and the corresponding dissipated charges (nanocoulomb), respectively.^{20,22} The charge is obtained by measuring the voltage (volt) across a 10 nF capacitor connected in series with the grounded plate. The area under this curve (loop) represents the power dissipated during the CH_4/N_2 plasma barrier discharge.^{4,5,20–22} The charge-voltage (Q-V) loop characteristic data has been taken for different plasma processing time. For a longer plasma deposition process the loop gets elongated in y-direction. This indicates that the charge density on the electrodes area increases with the deposition time. The dielectric constant of the reaction zone area also changes due to the thin film deposition on the electrodes. A typical Q-V loop corresponding to one discharge

cycle is shown in Fig. 2(b).²² It will help us to explain how to calculate the polarization as well as dielectric constant (at any instant) during the deposition process.²³

The capacitance is measured as the charge per unit voltage. We get the resultant charge as $(Q_{\text{max}} - Q_{\text{min}})$ and the voltage as $(V_{\text{max}} - V_{\text{min}})$ from Fig. 2. Since the applied voltage (V_{max}) is constant the quantities Q_{max} , Q_{min} , and V_{min} all vary with time. As a result the charge-voltage characteristic loop gets elongated in y-direction. The resulting change in capacitance of the system plays the key role in the measurement of the *in situ* dielectric constant of the deposited thin film. To make it clearer, we take the help of the basic formula of capacitance,

$$C = \frac{\epsilon_0 \epsilon_r A}{d}, \quad (4)$$

where ϵ_0 is the absolute permittivity of free space and ϵ_r is the dielectric constant of the medium. A is the area of the electrodes and d is the distance between the electrodes. Since the thickness of the deposited CN film ($\sim 1 \mu\text{m}$) is very much smaller (10^3 order) than the gas gap (that is 2 mm), d can be taken to be the same, before and after the film deposition. The typical film thickness after 5 h of deposition is about 6 to 10 μm . Electrode area A can also be taken to remain unchanged.

The polarization is given by the total charge per unit area and the dielectric constant as the ratio of two capacitances, one with the deposition and the other without the deposition. Thus we can calculate the values of P and ϵ_r from the following relations:

$$P = \frac{Q_{\text{max}} - Q_{\text{min}}}{\text{Area}}$$

and

$$\epsilon_{r(\text{equ})} = \frac{Q_{\text{max}} - Q_{\text{min}}/V_{\text{max}} - V_{\text{min}}}{C_{\text{DBD}}}, \quad (5)$$

where $\epsilon_{r(\text{equ})}$ stands for the equivalent dielectric constant of the DBD system. In our DBD system, the area of the elec-

trodes is 27.3 cm^2 and capacitance of the DBD system without deposition is 1.0087 nF . Using the values of Q_{\max} , Q_{\min} , V_{\max} , and V_{\min} as obtained from a particular loop of Fig. 2(a), we get the values of polarization and dielectric constant from the relations (8) at the corresponding plasma processing time. The total charge at the electrode surface is given by $Q(C) = V \times 10 \times 10 \text{ nC}$, where 10 is the probe factor and electrode being connected to ground via a 10 nF capacitor in series.

A pistol-grip IR thermometer has been employed to measure the electrode surface temperature from outside of the DBD chamber. The experimental results and the theoretically calculated temperature values have been compared and discussed later on.

III. THEORETICAL ASSUMPTION

All the observations are made at a pressure of 300 mbar (P_{ch}). The number density (n) in the reaction zone volume is given by

$$n = \frac{N_A}{V_S} \times \frac{P_{\text{ch}}}{P_0}, \quad (6)$$

where N_A is the Avogadro number and $V_S = 22\,400 \text{ cm}^3$ at $P_0 = 1000 \text{ mbar}$. Thus we get $n = 8.18 \times 10^{24} / \text{m}^3$. So, the effective mean kinetic energy density of the molecules at the reaction zone volume is

$$\langle E \rangle_{\text{effective}} = n \times \frac{3}{2} k_B (\Delta T), \quad (7)$$

where k_B = Boltzmann constant and ΔT is the temperature difference produced due to the corresponding physiochemical reactions. The temperature is the result of the average total kinetic energy of particles in matter.

Assuming the layer material to be linear and isotropic, its polarization (P) may be related to the electric field amplitude (E_0) by the relation,

$$P = \chi_e \epsilon_0 E_0 \quad \text{or} \quad P = \epsilon_0 (\epsilon_r - 1) E_0, \quad (8)$$

where $1 + \chi_e = \epsilon_r$ is the relative permittivity or the dielectric constant and $\epsilon_0 = 8.85 \times 10^{-12} \text{ F/m}$ is the absolute permittivity of free space and E_0 is the peak value of the applied electric field.

The ionized gas species or atoms/molecules are driven toward the electrodes' surface by the applied electric field. The applied electric field causes surface charge density to appear due to polarization. In some cases the particles become polarized and the local electric field is distorted. The mobility of the charges increases with increase in plasma treatment time. The migration of the mobile charges to areas with greatest field concentration results in increase of polarizability and the dipole moment. Every charge particle interacts according to its electronegativity and tries to rearrange themselves in polar and nonpolar orientations. These field induced dipoles attract one another and causes the particles to form chains or fibrous structures in the direction of the field. These chains are held together by inter particle forces that have sufficient strength to form a layer on the electrode surface.²⁴ Bulk polarization involves creation or alignment of molecular dipoles within the confines of the particular phase.

The frequency of collision increases at the surface of the electrodes due to accumulation of charge particles. Electrostatic field increases the aggregation of the particles at the surface of electrodes. The mean free path of the atoms gets reduced and ultimately becomes very small. According to our assumption, at equilibrium condition the effective mean kinetic energy of the atoms is equal to the electrostatic energy, so we can write

$$\langle E \rangle_{\text{effective}} = \frac{1}{2} \epsilon_0 |E_{\text{rms}}|^2 = \frac{1}{2} \epsilon_0 \frac{E_0^2}{2} \quad (9)$$

or

$$n \times \frac{3}{2} k_B (\Delta T) = \frac{1}{4} \epsilon_0 E_0^2, \quad (10)$$

where E_0 is the peak value of the applied electric field strength between the electrodes. From Eq. (8), we get the value of E_0 in terms of P and putting this value into Eq. (10), we get

$$\Delta T = \frac{1}{6 \rho \epsilon_0 k_B (\epsilon_{r(\text{equ})} - 1)^2} \times P^2. \quad (11)$$

Inserting the values of k_B , ϵ_0 , and the number density (n) of the reaction zone volume, we get

$$\Delta T = \frac{1.66 \times 10^8}{(\epsilon_{r(\text{equ})} - 1)^2} \times P^2. \quad (12)$$

Now, putting the corresponding value of P and ϵ_r as obtained from Eq. (5) and Fig. 2(a), in Eq. (11), we get the value of ΔT . Here, $\Delta T = T_{\text{Final}} - T_{\text{Room}}$ represents the difference in temperature. For example, if $\Delta T = 30 \text{ K}$ and $T_{\text{Room}} = 300 \text{ K}$, then the temperature of the electrode surface is $T_{\text{el}} = 330 \text{ K}$, i.e., $57 \text{ }^\circ\text{C}$. Thus we can calculate the temperature of electrode surface in our DBD system at any instant during hydrocarbon plasma deposition process.

IV. RESULTS AND DISCUSSIONS

Figure 3(a) shows the change of temperature with plasma deposition time. Calculation based on our assumption shows that the temperature varies from 70 to $43 \text{ }^\circ\text{C}$, whereas the experimentally obtained values vary from 58 to $42 \text{ }^\circ\text{C}$. Huge amount of heat is generated when breakdown discharge takes place (initial stage) and later on it approaches toward the thermodynamically stable state and it happens due to the formation of thin layer on the electrode surfaces. Once the layer starts to form, the local heat is absorbed and dissipated throughout the layer. This fact explains why the initial high temperature rapidly decreases with the increase in plasma processing time. The approximate error in the temperature measurement is $\pm 3 \text{ }^\circ\text{C}$. The temperature attains saturation value after about 5 h of deposition. The experimentally obtained temperature values are slightly smaller than the theoretical values due to the remote sensing processes of IR thermometer. Kersten *et al.*²⁵ mentioned that even an accurate knowledge of all the heat fluxes toward the substrate does not guarantee a good prediction of the surface temperature. It is therefore independently preferable to measure the temperature, e.g., by thermocouples or pyrometers

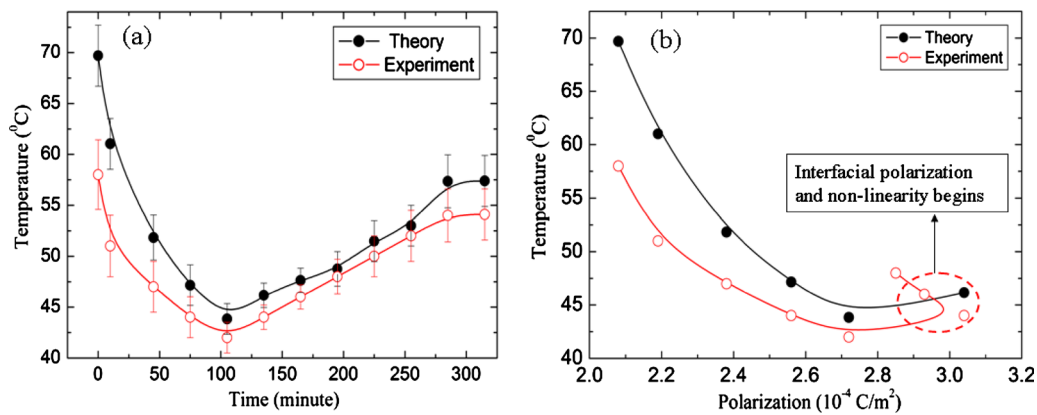


FIG. 3. (Color online) (a) Variations of electrode surface temperature with CH_4/N_2 (1:2) plasma deposition time. After 300 min of plasma processing, the temperature of the electrode surface attains saturation value. The vertical bars represent the error in measurement. (b) Temperature vs polarization curve. Red void circles represent the experimental values whereas black circles represent the theoretical values.

Figure 3(b) shows the variation of temperature with polarization during plasma processing. As expected physically, the polarization increases and the temperature decreases with time. Equation (12) indicates that the change in temperature depends on the changes in the values of both the polarization P and *in situ* dielectric constant of the deposited layer. Here we must point out that the linear theory as proposed here cannot be used to explain the phenomena in the interfacial polarization stage. Then one requires a nonlinear theory.

Figure 4 shows the temperature profile with respect to the dielectric constant of the deposited layer. Obviously, the change in temperature is affected by the change in the dielectric constant of the layer. As the film deposition is not uniform throughout the electrode surface, the dielectric property of the film becomes nonlinear. An important fact is that the interfacial polarization can involve migration of charge through the particles, along the surface, or within the double layer region of the dispersion. The change in polarization (dipolar or ionic) has strong impact on the dielectric relaxation of the deposited molecules. The anomalous change in

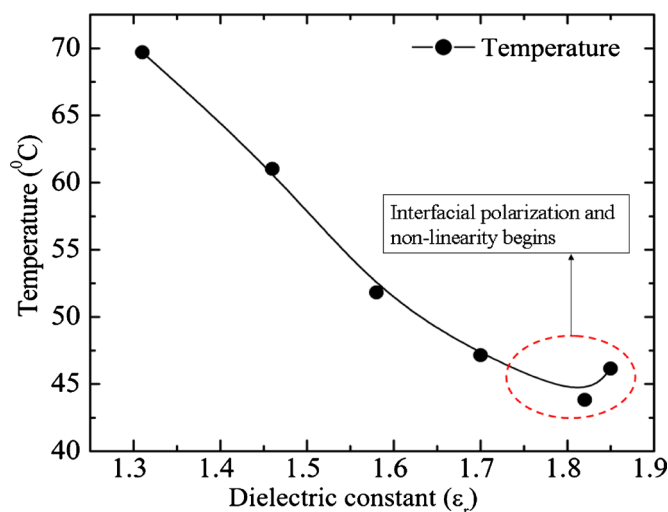


FIG. 4. (Color online) Variation of temperature of the electrode surface with the *in situ* dielectric constant of layer deposited by CH_4/N_2 (1:2) DBD plasma. This curve is plotted with the help of Eqs. (4) and (8).

temperature is observed when the dielectric constant changes from 1.8 to 1.9. Actually, it corresponds to a critical or transition point where the deposited layer drastically changes its property. At or beyond this point, our proposed relation (12) cannot be used. To describe such critical physical phenomenon, one requires a nonlinear theory because the plasma is basically nonlinear and at high values of electric field strength, the relation between polarization and electric field also becomes nonlinear.

Moreover, the abrupt change in the dielectric constant at a longer deposition time may be due to the interfacial polarization and the local dielectric relaxation of the deposited molecules. The polymerized molecules start to relax after the discharge is switched off. So one has to simultaneously consider the plasma polymerization and ablation (microetching) of deposited C–N layer.^{19,25,26} The plasma has a strong impact on the deposited layer and the main effects of the plasma on the exposed layer surface are (i) cleaning, (ii) ablation (microetching), (iii) crosslinking, and (iv) surface chemical functionalization. In this respect, the cleaning and ablation processes eliminate the weak boundary layer at the interface. Crosslinking due to energetic ultraviolet radiation rheologically stabilizes the interface, and the chemical functionalization may result in stronger covalent bonds between the coating and the polymer's backbone carbon via oxygen or nitrogen containing linkages.^{19,27} An interesting observation is that the C, H, and N layers are not homogeneous and consist of several intermixing layers and it is rather difficult to distinguish the boundaries of the layer. Intermixing happens due to the bulk polarization.^{13,18,23,27} Interfacial polarization involves the drift of carriers to or around a boundary that partially or totally retains charges, whereas the dipolar polarization involves the rotation of dipoles. The flat Q–V curve is due to the involvement of both interfacial and dipolar polarization.

The presence of any UV irradiation indirectly contributes to the formation of radicals through energy transfer of the photosensitizer.⁵ However, in the case of our DBD plasma power, dissipation is only about 3–10 W and the intensity of UV radiation produced is negligible. Some of the properties of the deposited film are influenced by the plasma

discharge parameters such as the applied electric field configuration, gap distance, gas mixture, pressure, etc. This is due to the fact that with a different discharge parameter, the gas fragmentation pattern or the ions and radical formation become different. For example, we find that at relatively high power dissipation level the deposited film thickness is higher than the corresponding low power value.

Electrons in the plasma transfer energy to the polymers through electrostatic interaction and then the ionization or excitation of the polymers occurs. The ionization leads to molecular fragmentation that contains small fragments with free radical. The excitation leads to the dissociation of the excited polymers and free radicals are formed.^{23,28–30}

As we are working at near atmospheric pressure discharge and the distance between the electrodes is small (2 mm), the collision rate is high some amount of thermal energy of the plasma is likely to be transferred to the electrodes. As pointed out in Sec. I, the inelastic collision in the active plasma volume and plasma-surface interactions is primarily responsible for the formation of polymers. However in our experimental setup “field induced dipoles” provide an additional mechanism for polymerization. In our system, the electric field between the electrodes is high (10^7 V/m) and at every discharge cycle the charge carriers move toward the electrode surface area according to their polarity. The field induced dipoles attract one another and also causes the particles to form chains or fibrous structures in the direction of the field. These chains are held together by inter particle forces that have sufficient strength to form a layer on the electrode surface. Thus the field induced dipoles provide an additional mechanism for polymerization.

V. CONCLUSION

We have developed a semiquantitative model to explain the measured variations of polarization and temperature at the electrode surface during DBD operation. The model correlates polarization and temperature with the dielectric constant of the deposited film. Although our model is based on a crude assumption the theoretically calculated temperatures are found to agree well with the experimental values. The electrode temperature during the CN layer deposition in CH_4/N_2 DBD plasma is found to be linearly proportional to the square of the polarization and inversely proportional to the square of the change in *in situ* dielectric constant from unity. The results presented in the paper may be helpful in the understanding of the mechanism of thin film deposition by means of DBD plasma. Such a study is important because at present the thin film deposition by means of DBD is a promising field in plasma technology. Finally, we would like to mention that our assumption is valid for hydrocarbons such as CH_4 , C_2H_4 , C_2H_6 , C_2H_2 , etc. but not for inert gases such as He, Ar, etc. The linear theory presented in the paper

cannot be used to explain the phenomenon in the interfacial polarization stage. Then one requires to develop a nonlinear theory.

ACKNOWLEDGMENTS

A part of this work was supported by the Deutsche Forschungsgemeinschaft (DFG) through Sonderforschungsbereich SFB/TR24 “Fundamentals of Complex Plasmas.” We take this opportunity to thank the reviewer for raising some pertinent physical questions and giving a number of constructive suggestions that helped to improve the presentation.

- ¹B. Hong, M. Wakagi, W. Drawl, R. Messier, and R. W. Collins, *Phys. Rev. Lett.* **75**, 1122 (1995).
- ²W. J. Gammon, G. L. Hoatson, B. C. Holloway, R. L. Vold, and A. C. Reilly, *Phys. Rev. B* **68**, 195401 (2003).
- ³N. Hellgren, M. P. Johansson, E. Broitman, L. Hultman, and J. E. Sundgren, *Phys. Rev. B* **59**, 5162 (1999).
- ⁴A. Majumdar, G. Das, K. R. Basvani, J. Heinicke, and R. Hippler, *J. Phys. Chem. B* **113**, 15734 (2009).
- ⁵A. Majumdar, J. Schäfer, P. Mishra, D. Ghose, J. Meichsner, and R. Hippler, *Surf. Coat. Technol.* **201**, 6437 (2007).
- ⁶W. Fukarek and H. Kersten, *J. Vac. Sci. Technol. A* **12**, 523 (1994).
- ⁷I. Herrmann, V. Bruser, S. Fiechter, H. Kersten, and P. Bogdanoff, *J. Electrochem. Soc.* **152**, A2179 (2005).
- ⁸A. Majumdar, M. Ganeva, D. Koepf, D. Datta, P. Mishra, S. R. Bhattacharyya, D. Ghose, and R. Hippler, *Vacuum* **83**, 719 (2009).
- ⁹A. Majumdar, G. Das, N. Patel, P. Mishra, D. Ghose, and R. Hippler, *J. Electrochem. Soc.* **155**, D22 (2008).
- ¹⁰H. Kersten and J. Winter, *Vacuum* **71**, 347 (2003).
- ¹¹G. Morfill and H. Kersten, *New J. Phys.* **5**, 2003 (2003).
- ¹²T. Farouk, B. Farouk, A. Gutsol, and A. Fridman, *J. Phys. D* **41**, 175202 (2008).
- ¹³A. von Keudell and W. Moeller, *J. Appl. Phys.* **75**, 7718 (1994).
- ¹⁴N. Mantzaris, E. Gogolides, A. Boudouvis, A. Rhallabi, and G. Turban, *J. Appl. Phys.* **79**, 3718 (1996).
- ¹⁵D. Herrebout, A. Bogaerts, M. Yan, and R. Gijbels, *J. Appl. Phys.* **90**, 570 (2001).
- ¹⁶M. Frenklach and H. Wang, *Phys. Rev. B* **43**, 1520 (1991).
- ¹⁷B. Yu and S. Girschick, *J. Appl. Phys.* **75**, 3914 (1994).
- ¹⁸M. Coltrin and D. Dandy, *J. Appl. Phys.* **74**, 5803 (1993).
- ¹⁹H. Yasuda, *J. Macromol. Sci., Chem.* **A10**, 383 (1976).
- ²⁰A. Majumdar and R. Hippler, *Rev. Sci. Instrum.* **78**, 075103 (2007).
- ²¹*Low Temperature Plasmas, Fundamentals, Technologies, Techniques*, edited by R. Hippler, H. Kersten, M. Schmidt, and K. H. Schoenbach (Wiley-VCH, Berlin, 2008), Vols. 1 and 2.
- ²²H. E. Wagner, R. Brandenburg, K. V. Kozlov, A. Sonnenfeld, P. Michel, and J. F. Behnke, *Vacuum* **71**, 417 (2003).
- ²³A. Majumdar, G. Scholz, and R. Hippler, *Surf. Coat. Technol.* **203**, 2013 (2009).
- ²⁴D. E. Hooks, T. Fritz, and M. D. Ward, *Adv. Mater. (Weinheim, Ger.)* **13**, 227 (2001).
- ²⁵H. Kersten and G. M. W. Kroesen, *Contrib. Plasma Phys.* **30**, 725 (1990).
- ²⁶H. Deutsch, H. Kersten, and A. Reutscher, *Contrib. Plasma Phys.* **29**, 263 (1989).
- ²⁷H. Deutsch, H. Kersten, S. Klagge, and A. Rutscher, *Contrib. Plasma Phys.* **28**, 149 (1988).
- ²⁸J. A. Thornton, *J. Vac. Sci. Technol.* **11**, 666 (1974).
- ²⁹H. Kersten, H. Steffen, D. Vender, and H. E. Wagner, *Vacuum* **46**, 305 (1995).
- ³⁰H. Kersten, R. J. M. M. Snijkers, J. Schulze, G. M. W. Kroesen, H. Deutsch, and F. J. Dehoog, *Appl. Phys. Lett.* **64**, 1496 (1994).